

ChemComm

Accepted Manuscript



This is an *Accepted Manuscript*, which has been through the Royal Society of Chemistry peer review process and has been accepted for publication.

Accepted Manuscripts are published online shortly after acceptance, before technical editing, formatting and proof reading. Using this free service, authors can make their results available to the community, in citable form, before we publish the edited article. We will replace this *Accepted Manuscript* with the edited and formatted *Advance Article* as soon as it is available.

You can find more information about *Accepted Manuscripts* in the [Information for Authors](#).

Please note that technical editing may introduce minor changes to the text and/or graphics, which may alter content. The journal's standard [Terms & Conditions](#) and the [Ethical guidelines](#) still apply. In no event shall the Royal Society of Chemistry be held responsible for any errors or omissions in this *Accepted Manuscript* or any consequences arising from the use of any information it contains.

COMMUNICATION

Supramolecular Design of Low-dimensional Carbon Nano-hybrids encoding a Polyoxometalate-bis-Pyrene Tweezer

Cite this: DOI: 10.1039/x0xx00000x

Received 00th January 2012,
Accepted 00th January 2012Gloria Modugno,^a Zois Syrgiannis,^b Aurelio Bonasera,^b Mauro Carraro,^a Gabriele Giancane,^c Ludovico Valli,^{*c} Marcella Bonchio,^{*a} and Maurizio Prato^{*b}

DOI: 10.1039/x0xx00000x

www.rsc.org/

A novel bis-pyrene tweezer anchored on a rigid polyoxometalate scaffold fosters a unique interplay of hydrophobic and electrostatic supramolecular interactions to shape CNS-based extended architectures.

Nanoscience innovation can be pursued with supramolecular touch, by the controlled self-assembly of molecular building blocks. One key goal is the encoding of a diversity-oriented strategy, to tune composition, structure and final morphology of the emerging materials shaped and grown at the nano-scale.^{1,2} Success in this task rests on the choice of tailored molecular components, displaying some complementary interaction patterns, tunable on request and with adaptive response to the evolving system.¹

We have recently shown how carbon nanostructures (CNS) can evolve to functional nano-hybrids anchoring inorganic polyoxometalates (POM) by electrostatic interactions. High POM loading is obtained by providing the CNS with a vast array of surface-appended ammonium groups through the covalent insertion of tetra-alkyl PAMAM dendrimers,^{3,4} or *N,N,N*-trimethylbenzene ammonium residues.⁵ Although multiple and complementary electrostatic interactions can guarantee stable POM-CNS composites, additional hydrophobic and π - π forces can be instrumental to control the spatial organization and order of the resulting supramolecular assembly.⁵ We have thus equipped the inorganic POM unit with a pyrene-tweezer receptor as a molecular recognition tool for CNS. Hybrid POMs with pendant pyrene groups were proposed for the construction of supramolecular and functional assemblies.⁶⁻⁸ Indeed, the extended π -system of the pyrene moiety can bind to hydrophobic/aromatic molecules, including fullerenes and carbon nanotubes (CNTs).^{9,10} With this aim, a novel Keggin decatungstosilicate featuring a covalent bis-pyrene functionality has been synthesized and used in combination with CNS to design supramolecular nano-hybrids with 0-, 1- or 2-D morphology (Figure 1). Pyrene-tagged $(\text{Bu}_4\text{N})_4\{[(\text{C}_{16}\text{H}_9)\text{SO}_2\text{NH}(\text{CH}_2)_3\text{Si}]_2\text{O}(\gamma\text{-SiW}_{10}\text{O}_{36})\}$ (**1**) is obtained (70% yield) from the parent bis-aminopropylsilane derivative upon its post functionalization with pyrene sulfonyl chloride, in the presence of triethylamine, at 50°C in CH_3CN (see Scheme S1, ESI†).¹¹ **1** was characterized by heteronuclear NMR, FT-IR, ESI-MS, UV-Vis, zeta-potential analysis and fluorescence spectroscopy (Figures S1-S8, ESI†). In particular, ESI-

MS (negative mode, CH_3CN) yields two peaks at $m/z = 789.5$ and 1053.1, ascribed to the tetra-anionic species $([\text{C}_{38}\text{H}_{32}\text{N}_2\text{O}_{41}\text{S}_2\text{Si}_3\text{W}_{10}]^{4-}, m/z = 789.9)$ and to its mono-protonated form ($m/z = 1053.5$). ^{183}W NMR (CD_3CN) signals at -107.51 (4 W), -136.03 (2W), -141.52 (4 W) ppm confirm the expected C_{2v} symmetry resulting from a bis-functionalization of the POM surface.¹²

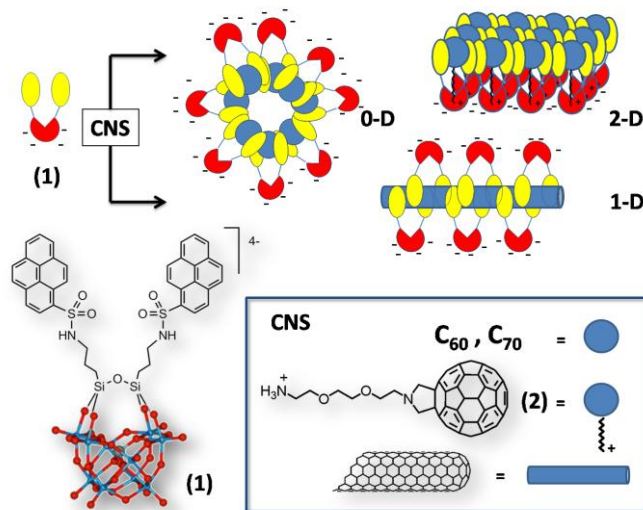


Figure 1 Structure of POM **1** evolving to 0-, 1-, 2-D supramolecular assemblies upon CNS binding.

The tweezer-type arrangement of the facing aromatic moieties, sets a sp^2 -all-carbon lattice for the supramolecular association with CNS through π - π stacking and van der Waals forces.^{13,14} The receptor properties of **1** have been initially assessed with C_{60} as molecular guest, by spectrophotometric titration experiments. When C_{60} (*o*-DCB, 5×10^{-3} M, 4 μL aliquots) is added to a DMF solution of **1** (10 μM), modification of the UV-Vis spectrum is observed due to a steady enhancement of the absorption bands in the range 330-370 nm, involving the $\pi \rightarrow \pi^*$ transitions of both chromophores (Figure

S9).¹⁵ A host-guest π - π interaction is confirmed by the analysis of the pyrene emission upon binding of C_{60} . The fluorescence spectrum of **1** (10 μ M in DMF, λ_{exc} = 338nm) shows the typical pattern of the pyrene fluorophore, with two bands centered at 379 and 397 and a shoulder around 416 nm.¹⁶ The weak excimer emission, observed at 450-500 nm, indicates a pyrene-driven aggregation of **1**, via π - π stacking of the aromatic domains in the high polar DMF environment.¹⁷ Addition of C_{60} has a major effect on emission by **1**, causing a strong luminescence decrease in all range of frequencies (Figure S9, ESI[†]).^{15,18} Monitoring of the fluorescence intensity ratio, $(I_0/I)-1$, at 397 nm, yields a linear Stern-Volmer (SV) plot, as a function of added C_{60} (up to 3 equivalents, Figure 2a).

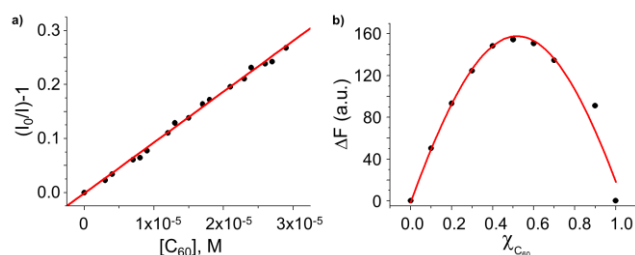


Figure 2 a) Fluorimetric Stern-Volmer graph (λ_{exc} = 350 nm; λ_{em} = 397 nm) obtained for **1** (10 μ M) upon addition of C_{60} (10^{-3} M in *o*-DCB) and (b) Job plot for **1** and C_{60} in DMF/*o*-DCB (T=298 K).

The resulting binding constant, $K_{sv} = 9.40 \times 10^3 \text{ M}^{-1}$, is consistent with a pyrene-driven host-guest interaction¹⁹ (data were corrected for the inner filter absorption effects of the C_{60} , see ESI[†]). Noteworthy, addition of water (1% H_2O in DMF) promotes C_{60} binding, yielding a steeper SV-slope and an increase of the association constant ($K_{sv} = 3.54 \times 10^4 \text{ M}^{-1}$), by virtue of a reinforced hydrophobic interaction (Figure S11, ESI[†]). Binding of C_{70} (Figures S10 and S12, ESI[†]) occurs with a $K_{sv} = 9.83 \times 10^4 \text{ M}^{-1}$, showing a one order of magnitude increase of the supramolecular interaction with the bis-pyrene tweezer. This is likely due to the larger π -area of the C_{70} guest and to the adjustable flexibility of the bis-pyrene receptor arms.^{20,21} The stoichiometry of the fullerene/**1** complexes has been determined for both C_{60} and C_{70} guests with Jobs plot of the continuous variation method. It turns out that fullerenes bind **1** in a 1:1 fashion (Figures 2b and S13, ESI[†]). 0-D globular particles can be observed by Transmission Electron Microscopy (TEM) with dimensions in the range 200-700 nm (Figures S14 and S15, ESI[†]).

The hydrophobic self-assembly of the fullerene core with **1**, as encoding structural block, has been further investigated at the air-water interface by the organization of 2-D Langmuir films. With this aim, the amphiphilic fulleropyrrolidine **2** was used instead of pristine C_{60} . Compound **2** displays a hydrophobic fullerene core bearing a triethylene glycol chain terminated with an ammonium group, thus suitable to drive the aggregation in aqueous media.²² The assembly properties of **2** at the air-water interface are readily screened by means of Langmuir curves and Brewster angle microscopy (BAM). The surface pressure vs area isotherm of Langmuir films were recorded at a barrier rate of $3.9 \text{ \AA}^2 \text{ mol}^{-1} \text{ min}^{-1}$, thus enabling the characterization of the supramolecular arrangement of the floating molecular layers (Figure S17, ESI[†]). Initially, fulleropyrrolidine **2** was dissolved in chloroform (0.13 mg ml^{-1}) and spread (150 \mu L) on the ultrapure water surface. The same procedure was repeated on a water surface containing **1** (10^{-6} mol/L). In this latter case, the origination of a supramolecular organization is apparent from the Langmuir curve modification, yielding a marked shift towards higher limiting area values, and suggesting the binding to the pyrene-tweezer. Images of the floating film at Brewster angle shed light on interphase events (Figure 3 and Table S1).²³ Indeed **2** as

floating layer over the POM-containing sub-phase yields a 2-D array of aggregates (Figure 1) that coalesce upon compression at increasing pressure. This is not the case in the absence of **1**, where the interface coverage is unorganized and not affected by the applied pressure (Figure 3).²⁴

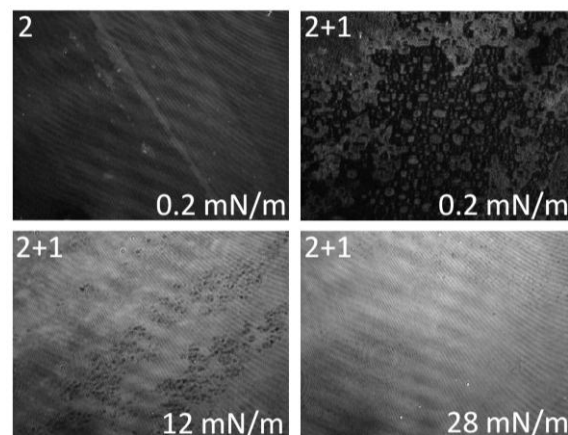


Figure 3 Brewster angle microscopy (BAM) images recorded at different surface pressure. Top, left: fulleropyrrolidine **2** (image taken at 0.2 mN/m); other images were taken at increasing surface pressure (0.2÷28 mN/m) for the **2/1** system. BAM images are 430 nm in width.

The supramolecular film with assembled **2** and **1** components is readily transferred on ITO or gold substrates by means of the Langmuir-Schaefer method, i.e., the horizontal variation of the Langmuir-Blodgett technique, with accurate control of the deposition parameters.^{25,26} FT-IR analysis confirms the simultaneous transfer of both building blocks within the layered 2-D assembly (Figure 1) thus providing clear evidence of the host-guest interlocking surface arrays (Figure S16, ESI[†]).

The binding affinity of **1** towards low dimensional carbons has been exploited to yield stable dispersions of SWCNTs (HiPco tubes), upon sonication in DMF (1h at room temperature), followed by centrifugation (1h at 1000 rpm). The resulting supernatant dispersion of **1**@HiPco tubes was separated from the precipitate, analysed by UV-Vis-NIR absorption and fluorescence spectroscopies, and compared to the one obtained with HiPco tubes solubilized using sodium dodecyl sulfate (SDS) in D_2O (Figure 4a). For a more precise spectral comparison, **1**@HiPco composite was filtered and washed several times with acids and bases in order to remove the inorganic complex **1** (*r*-HiPco), and then re-suspended in SDS/ D_2O (Figure 4, blue line). The UV-Vis-NIR pattern of the SWCNT suspension confirms the key role of the bis-pyrene tweezer to act as a dispersant, providing the carbon surface with a polyanionic “coating” (Figure 1). The anionic charge of **1**@HiPco is corroborated by zeta-potential analysis, which turns out as low as -13 mV. Quenching of emission was observed for **1**@HiPco with respect to **1** alone (Figure S18, ESI[†]).²⁷ Further characterization of the **1**@HiPco association is provided by Raman spectra, where all the characteristic features of the SWCNTs are evident (Figure S19, ESI[†]). In particular, analysis of the radial breathing-mode (RBM) region, with excitation at $\lambda=633 \text{ nm}$, allows the identification of bands arising from both semiconducting and metallic nanotubes. A small hypsochromic shift of all the Raman features (ca 4 nm, at different laser excitation) results upon complexation of SWCNT with **1** (compare black and red lines in Figures 4b and S19, ESI[†]), which is consistent with the electronic interaction between the two

components. The original Raman shifts are restored upon extensive washing to remove the inorganic domain (*r*-HiPco, blue line in Fig 4b). Modification of the RBM region intensity can be associated to some preferential binding with SWCNTs of different diameters/chirality patterns.²⁸ In order to highlight any modification due to selective recognition by **1**, the normalized RBM signals were also registered upon excitation at 532 nm and 785 nm (Figure S19, ESI†). From the collection of Raman spectra, it is apparent that the pyrene-based tweezer shows a preferential interaction with large diameter tubes, that undergo a substantial enrichment in the suspension with respect to the smaller ones (compare Figures S19-S20, ESI†).

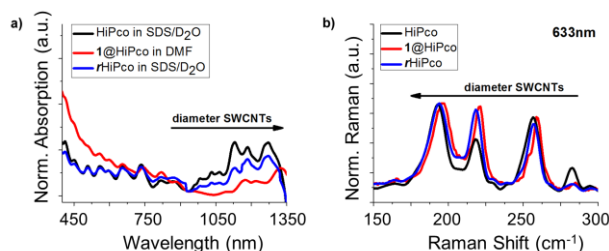


Figure 4 a) Normalized UV-Vis-nIR spectra of **1**@HiPco in DMF in comparison with HiPco and *r*HiPco spectra recorded in 1% SDS in D₂O. (b) Normalized RBMs of p-SWCNT (as-received), **1**@HiPco and *r*HiPco. Excitation wavelength = 633 nm.

This result is in agreement with the observed C₇₀/C₆₀ selectivity ratio discussed above, and is likely to be amplified by multiple interaction sites on the 1-D nanostructures. As a corollary information, thermogravimetric analysis (TGA) of **1**@HiPco shows a weight loss of 17%, corresponding to a 69 μmol/mg POM loading (Figure S23, ESI†), while TEM and AFM images confirm the expected 1-D morphology of the hybrid nano-composites (Figure S24 and S25, ESI†).

Conclusions

In summary, the tweezer arrangement of the bis-pyrene unit combined with a totally inorganic and robust POM framework holds a promising potential for CNS separation and processing. Evolution of the supramolecular assembly driven by the pyrene-based receptor from nano to meso-scale arrangement is herein demonstrated on 2-D surfaces.

Financial support from Fondazione Cariparo (Nanomode Progetti di Eccellenza 2010), MIUR (PRIN contract No. 2010N3T9M4, FIRB RBAP11C58Y, FIRB RBAP11-ETKA_006), FP7-SACS-2013 project, is gratefully acknowledged. We acknowledge the participation in the ESF COST action 1203 (PoCheMoN).

Notes and references

^a CNR-ITM and Department of Chemical Sciences, University of Padova, via F. Marzolo 1, 35131 Padova, Italy.

^b Center of Excellence for Nanostructured Materials (CENMAT) and INSTM, unit of Trieste, Department of Chemical and Pharmaceutical Sciences, University of Trieste, Piazzale Europa 1, 34127 Trieste, Italy.

^c Department of Biological and Environmental Sciences and Technologies, DISTEBA University of Salento Via per Arnesano, I-73100 Lecce, Italy.

Electronic Supplementary Information (ESI) available: synthetic and analytical procedures, Langmuir films. See DOI: 10.1039/c000000x/

- H. Imahori and T. Umeyama, *J. Phys. Chem C*, 2009, **113**, 9029.
- F. D'Souza and O. Ito, *Chem. Soc. Rev.*, 2012, **41**, 86.
- F. M. Toma, A. Sartorel, M. Iurlo, M. Carraro, P. Parris, C. Maccato, S. Rapino, B. R. Gonzalez, H. Amenitsch, T. Da Ros, L.

- Casalis, A. Goldoni, M. Marcaccio, G. Scorrano, G. Scoles, F. Paolucci, M. Prato and M. Bonchio, *Nat. Chem.*, 2010, **2**, 826.
- M. Quintana, A. M. López, S. Rapino, F. M. Toma, M. Iurlo, M. Carraro, A. Sartorel, C. MacCato, X. Ke, C. Bittencourt, T. Da Ros, G. Van Tendeloo, M. Marcaccio, F. Paolucci, M. Prato and M. Bonchio, *ACS Nano*, 2013, **7**, 811.
- F. M. Toma, A. Sartorel, M. Iurlo, M. Carraro, S. Rapino, L. Hooper-Burkhardt, T. Da Ros, M. Marcaccio, G. Scorrano, F. Paolucci, M. Bonchio and M. Prato, *ChemSusChem*, 2011, **4**, 1447.
- D. Li, J. Song, P. Yin, S. Simotwo, A. J. Bassler, Y. Aung, J. E. Roberts, K. I. Hardcastle, C. L. Hill and T. Liu, *J. Am. Chem. Soc.*, 2011, **133**, 14010.
- Y. F. Song, D. L. Long and L. Cronin, *Angew. Chem. Int. Ed.*, 2007, **46**, 3900.
- B. Matt, C. Coudret, C. Viala, D. Jouvenot, F. d. r. Loiseau, G. Izzet and A. Proust, *Inorg. Chem.*, 2011, **50**, 7761.
- R. Vaiyapuri, B. W. Greenland, J. M. Elliott, W. Hayes, R. A. Bennett, C. J. Cardin, H. M. Colquhoun, H. Etman and C. A. Murray, *Anal. Chem.*, 2011, **83**, 6208.
- T. Ogoshi, Y. Takashima, H. Yamaguchi and A. Harada, *J. Am. Chem. Soc.*, 2007, **129**, 4878.
- M. Carraro, G. Modugno, G. Fiorani, C. Maccato, A. Sartorel and M. Bonchio *Eur. J. Org. Chem.* **2012**, 281.
- M. Carraro, L. Sandei, A. Sartorel, G. Scorrano and M. Bonchio, *Org. Lett.* 2006, **8**, 3671.
- C. Romero-Nieto, R. García, M. Á. Herranz, C. Ehli, M. Ruppert, A. Hirsch, Dirk M. Guldi and N. Martín *J. Am. Chem. Soc.* 2012, **134**, 9183.
- C. Romero-Nieto, R. García, M. Á. Herranz, L. Rodríguez-Pérez, M. Sánchez-Navarro, J. Rojo, N. Martín and Dirk M. Guldi *Angew. Chem. Int. Ed.* 2013, **52**, 10216.
- J. Xiao, Y. Liu, Y. Li, J. Ye, Y. Li, X. Xu, X. Li, H. Liu, C. Huang, S. Cui and D. Zhu, *Carbon*, 2006, **44**, 2785.
- J. González-Benito, J. C. Cabanelas, A. Aznar, M. R. Vigil, J. Bravo, B. Serrano and J. Baselga, *J. Lumin.*, 1997, **72-74**, 451
- Winnik, F. M. *Chem. Rev.* 1993, **93**, 587.
- M. I. Sluch, I. D. W. Samuel and M. C. Petty, *Chem. Phys. Lett.*, 1997, **280**, 315.
- Y. L. Hwang and K. C. Hwang, *Fullerene Sci. Techn.*, 1999, **7**, 437.
- S. Mukherjee, A. K. Bauri and S. Bhattacharya, *Spectrochim. Acta A*, 2010, **77**, 64.
- J. Yoo, Y. Kim, S.-J. Kim and C.-H. Lee, *Chem. Commun.*, 2010, **46**, 5449.
- V. Georgakilas, F. Pellarini, M. Prato, D. M. Guldi, M. Melle-Franco and F. Zerbetto, *PNAS*, 2002, **99**, 5075.
- V. Sgobba, G. Giancane, S. Conoci, S. Casilli, G. Ricciardi, D. M. Guldi, M. Prato and L. Valli, *J. Am. Chem. Soc.*, 2007, **129**, 3148.
- A. Montellano Lopez, A. Mateo-Alonso and M. Prato, *J. Mater. Chem.*, 2011, **21**, 1305.
- E. Vittorino, G. Giancane, S. Bettini, L. Valli and S. Sortino, *J. Mater. Chem.*, 2009, **19**, 8253.
- E. Vittorino, G. Giancane, D. Manno, A. Serra, L. Valli and S. Sortino, *J. Colloid Interf. Sci.*, 2012, **368**, 191.
- Y.-Y. Ou and M. H. Huang, *J. Phys. Chem. B*, 2006, **110**, 2031.
- R. Graupner, *J. Raman Spectrosc.*, 2007, **38**, 673.

COMMUNICATION

Supramolecular Design of Low-dimensional Carbon Nano-hybrids encoding a Polyoxometalate-bis-Pyrene Tweezer

Gloria Modugno, Zois Syrgiannis, Aurelio Bonasera, Mauro Carraro, Gabriele Giancane, Ludovico Valli, Marcella Bonchio, and Maurizio Prato

The host-guest chemistry of the POM-tweezer drives self-assembly with carbon nanostructures in the nano- to micro-scale yielding 0-,1-, and 2-D nano-hybrids.

